

Mode II Interlaminar Failure Mechanisms in Carbon Fibre / PEEK and Carbon Fibre / Epoxy Composites

Rozli Zulkifli
Wesley J. Cantwell
Matt Blyton

ABSTRACT

The mode II interlaminar fracture properties of two high performance composites have been examined in detail. The failure mechanisms occurring in these materials are investigated using the double end-notched flexure (DENF) geometry. Tests have been undertaken at crosshead displacement rates between 0.1 mm/minute and 3m/s and the failure mechanisms investigated in the scanning electron microscope. Detail studies of the crack tip regions in the DENF specimens showed that the amount and nature of damage depended strongly on the rate at which the specimen was deformed. At low loading rates, the crack tip damage zone in carbon fibre reinforced PEEK was very large extending on planes above and below that of the starter defect. At high rates of loading, damage was confined to the resin-rich region immediate to the crack tip. Similar observations were made in the carbon fibre/epoxy composite where large shear cracks were evident at low rates of loading and an array of microcracks at high rates.

ABSTRAK

Sifat patah antara lamina mod II bagi bahan komposit prestasi tinggi telah dikaji dengan terperinci. Mekanisme kegagalan yang berlaku dalam bahan ini telah dikaji menggunakan geometri lentur akhir-takukan dua. Ujian telah dijalankan pada kadar kecepatan antara 0.1 mm/minit dan 3 m/s dan mekanisme kegagalan dikaji dengan mikroskop imbasan elektron. Kajian terperinci pada bahagian hujung rekahan dalam spesimen tersebut menunjukkan nilai dan jenis kerosakan sangat bergantung pada kadar dimana spesimen diubah bentuk. Pada kadar pembebanan rendah, zon kerosakan pada hujung rekahan dalam PEEK bertetulang gentian karbon adalah sangat besar dan bersambung pada satah atas dan bawah kecacatan permulaan. Pada kadar pembebanan tinggi, kerosakan adalah terhad pada kawasan yang penuh dengan matrik/damar. Pemerhatian yang sama dibuat pada komposit gentian karbon/epoxy dimana rekahan ricih yang besar dapat dilihat pada kadar pembebanan yang rendah dan terdapat tatasusunan mikrorekahan pada kadar tinggi.

INTRODUCTION

Delamination is undoubtedly the most serious mode of failure in high performance composite materials such as those currently finding use in the aerospace industry. Interlaminar crack extension can occur under opening (mode I), shearing (mode II), tearing (mode III) or any combination thereof,

Figure 1. The first generation of composite materials based on brittle thermosetting polymer matrices offered fracture energies as low as 100 J/m^2 . The development of toughened thermosets and a wide range of high performance thermoplastics have seen this value increase to 2000 J/m^2 and beyond (Hashemi et al. 1990; Sue et al. 1993 and Yee 1986).

The polymer matrices used in high performance composite materials are likely to exhibit viscoelastic characteristics in which key physical properties such as yield stress, strain to failure and fracture toughness are dependent upon both test temperature and strain rate (Bradsky et al. 1993, Cantwell and Morton 1989). The way in which fibre reinforced plastics respond to high strain rates is of particular interest since work has shown that localised impact loading can generate large areas of interlaminar fracture (Wang 1995). A number of researchers have examined the influence of varying loading rate on the interlaminar fracture toughness of aerospace grade composites. Yaniv and Daniel (1988) conducted high rate mode I fracture tests on a relatively brittle matrix composite and found that the mode I fracture energy G_{IC} first increased and then decreased with increasing crack velocity. Todo et al. (1997) tested four different woven fabric polyamide composites under mode I loading conditions with two kinds of reinforcements, carbon fibre and glass fibre. The results showed that both tensile strength and failure strain of these composites tend to increase with increase of strain rate.

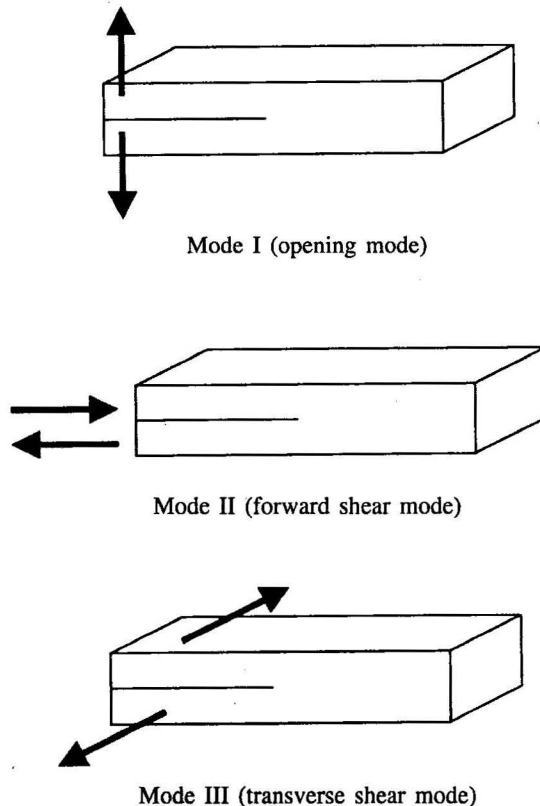
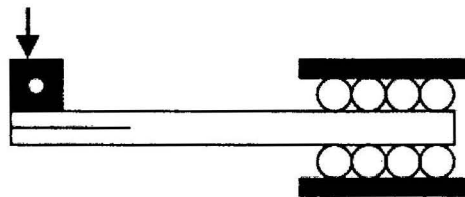


FIGURE 1. Schematic showing the modes of deformation in cracked body

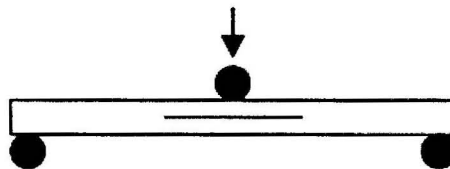
Only a few researchers have studied the mode II interlaminar fracture properties of composites at high rates of strain. Figures 2a to 2c show typical specimen geometries used for characterising the mode II interlaminar fracture toughness of composite materials. Maikuma et al. (1990) used the CNF geometry, Figure 2b, and showed that the G_{IIC} of unidirectional AS4 carbon fibre reinforced PEEK dropped by roughly twenty percent at high loading rates. However, very little is known about the failure mechanisms occurring during interlaminar failure. Maikuma et al. (1990) used a scanning electron microscope to examine the fracture surfaces of their PEEK matrix composites. They found that the quasi-static fracture surfaces exhibited ductile tearing whereas little plastic deformation was in evidence at dynamic rates of loading.

The aim of the present work was to investigate the interlaminar failure mechanisms occurring in two carbon fibre reinforced plastics over wide range of loading rates using ENF and DENF specimen geometries. The findings will then be correlated with mode II interlaminar fracture data for this material.

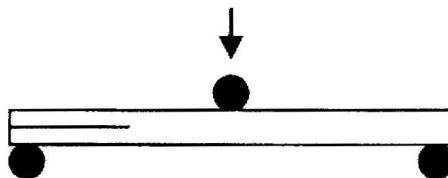


(a) End-loaded split (ELS) geometry

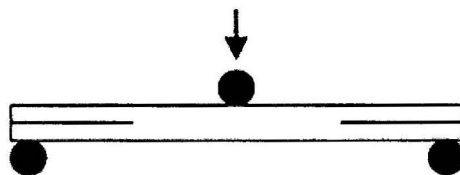
perpustakaan
Fakulti Kejuruteraan
Universiti Kebangsaan Malaysia



(b) Centre-notched flexure (CNF) geometry



(c) End-notched flexure (ENF) geometry



(d) Double end-notched flexure (DENF) geometry

Figure 2. Typical mode II test geometries

EXPERIMENTAL PROCEDURES

Initial tests were undertaken using the End-Notched Flexure (ENF) specimen shown in Figure 2c (Davies 1990). Two materials were examined in this study: (1). Three millimetre thick panels of carbon fibre reinforced PEEK were manufactured by compression moulding unidirectional prepegs in a press at 380°C. (2). Four millimetre thick woven carbon fibre reinforced epoxy resin panels were moulded according to the manufacturer's specifications. Folded aluminium starter defects were incorporated into the end of each panel. Specimens with dimensions 100 mm x 15 mm were removed from the panels using a diamond slitting wheel. Three point bend tests were undertaken on a screw-driven INSTRON 1122 universal testing machine at rates of 0.1 mm/min, 1.0 mm/min, 10 mm/min, 100 mm/min and 3 m/s.

Since the response time of the load cell was not considered to be sufficient for the tests at 100 mm/min and 3 m/s, a piezo-electric load cell connected to a UPM60 high speed data logger was used. Impact testing was conducted on an instrumented drop-weight tower. Here, load was measured using the aforementioned load cell and data logger, and displacement using an optical extensometer system consisting of an optical fibre positioned on the carriage and a transducer located directly behind it. A thin piece of rubber was placed at the impact location to reduce ringing effects in the load cell. Frictional effects between the upper and lower crack surfaces were minimized by placing a 100 µm thick piece of Teflon film close to the crack tip. This was found to be extremely important since failing to do so resulted in measured values of G_{IIC} some 33% higher than in cases where Teflon was included. The mode II strain energy release rate was calculated according to the beam theory compliance method, where :

$$G_{IIC} = \frac{9P^2a^2}{16B^2Eh^3} \quad (1)$$

where h is the specimen half thickness, B is the specimen width, a is the initial crack length and P is the applied force (in this case the maximum force). The elastic modulus, E , was measured on an unnotched specimen at the appropriate strain rate.

Failure mechanisms were investigated using the double end-notched flexure (DENF) specimen, Figure 3. The specimen dimensions were 140 x 15 mm. The detailed experimental procedures for preparing the specimen for scanning electron microscopy are described by Sue (1990) but a brief description is given here. The specimen edges were ground and subsequently polished on a rotating wheel using a one micron paste. In preparation for subsequent examination in the scanning electron microscope, a thin layer of gold was sputtered onto one of the specimen edges prior testing. Three point bend tests were conducted at crosshead displacement rates of 0.1, 1, 10, 100 and 3m/s. The tests were stopped once an unstable crack had propagated from one of the aluminium starter defects. The fracture surfaces in the failed half of the specimen and the crack tip region in the unfailed section were then examined individually in a Hitachi scanning electron microscope. This approach enabled the failure mechanisms occurring at the crack tip just prior

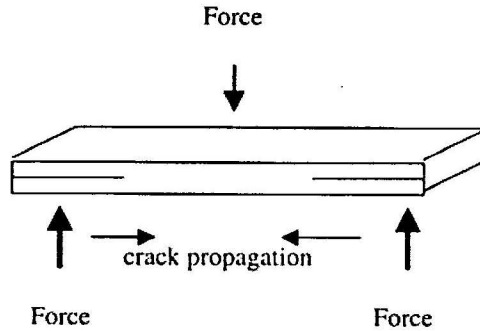


FIGURE 3. Crack propagation in Double end-notched flexure (DENF) geometry

to failure to be correlated with the features apparent on the fracture surface immediately after failure.

RESULTS AND DISCUSSION

Figure 4 shows the variation of G_{IIC} with crosshead displacement rate for the carbon fibre reinforced PEEK composite calculated using the beam theory compliance method.

The data clearly indicate that the interlaminar fracture toughness of this material increases rapidly with loading. However, Smiley and Pipes (1987) observed a dramatic loss in interlaminar fracture properties at higher rates of loading. Similar trends are apparent in the mode II fracture data for the woven carbon fibre reinforced epoxy laminate, Figure 5. A comparison of Figures 4 and 5 indicates that the woven carbon fibre reinforced epoxy exhibits an interlaminar fracture toughness comparable to that offered by the thermoplastic laminate.

In an attempt to explain the experimental trends apparent in Figures 4 and 5, the crack tip failure mechanisms were examined using the DENF

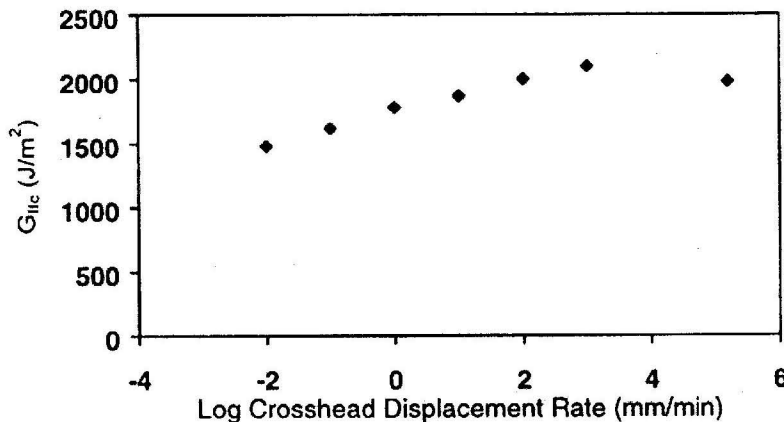


FIGURE 4. Variation of G_{IIC} with loading rate for the carbon fibre reinforced PEEK composite.

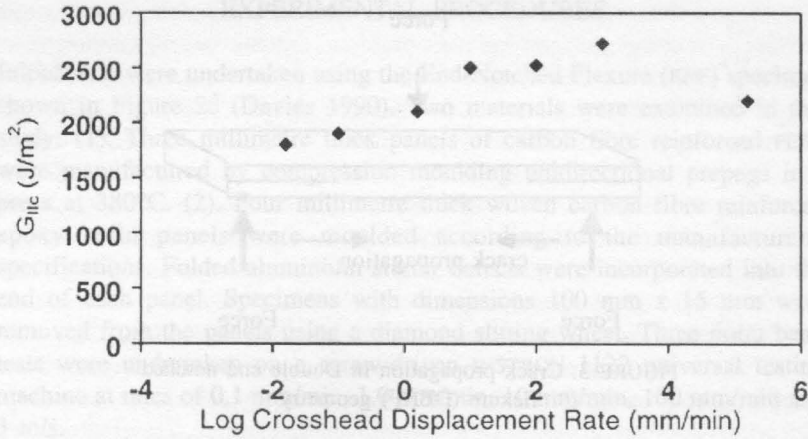


FIGURE 5. Variation of G_{IIc} with loading rate for the woven carbon fibre reinforced epoxy.

geometry. Figures 6 and 7 show the crack tip region in the unfractured half of a carbon fibre reinforced PEEK specimen tested at 1 and 10 mm/minute. The aluminium starter defect is clearly visible on the left hand side of the micrograph. The photograph clearly indicates the presence of localized cracking in the resin-rich zone in front of the defects as well as the fibre-

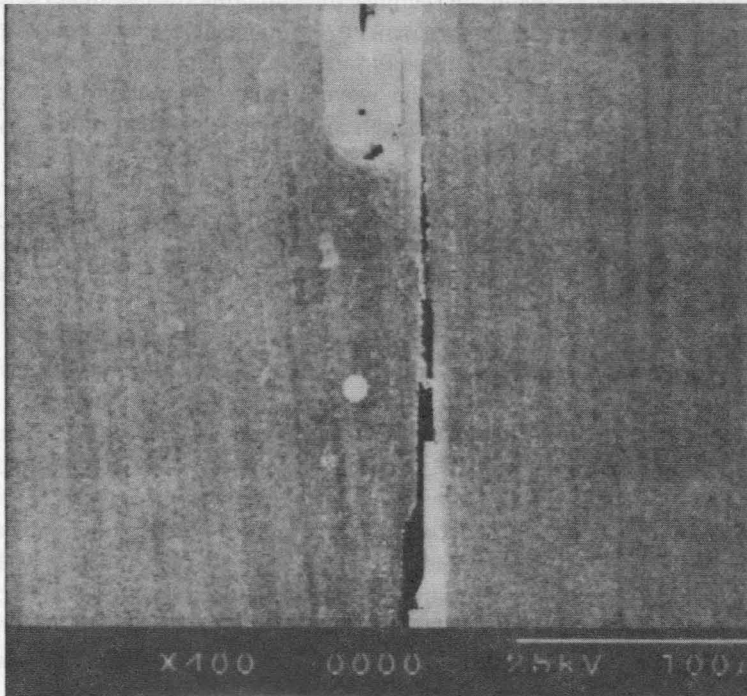


FIGURE 6. Crack tip region in a carbon fibre reinforced PEEK specimen tested at 1.0 mm/min

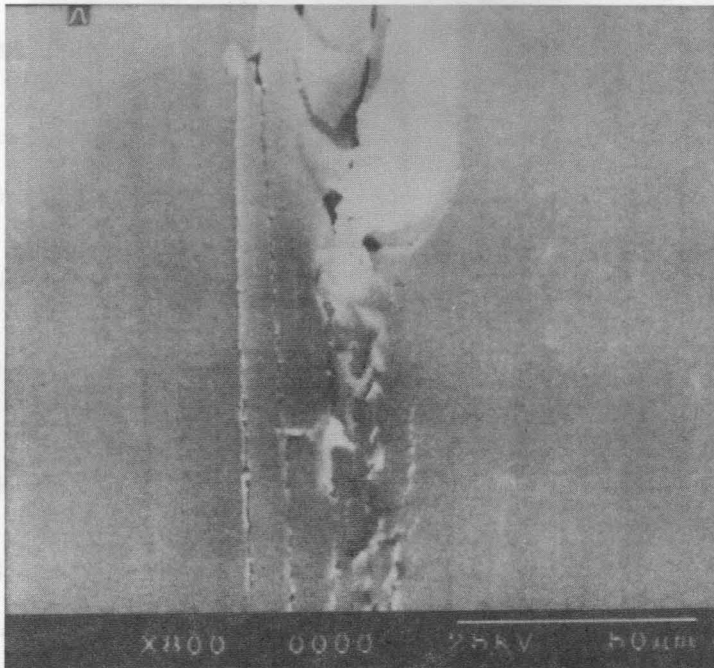


FIGURE 7. Crack tip region in a carbon fibre reinforced PEEK specimen tested at 10 mm/min

matrix interface just below the level of the defect. Microcracking in the specimen tested at a crosshead displacement rate of 0.1 mm/minute was more extensive, propagating on planes well above and below that of the starter defect. At loading rates of 10 mm/minute and above, damage was confined to the resin-rich region immediately in front of the aluminium defect. Figure 8 shows the crack tip region in a specimen loaded under impact conditions. A detailed examination of this region indicated that damage was limited to the region immediately ahead of the starter defect. The figure highlights the presence of a fine array of microcracks in the resin-rich area. It is believed that these microcracks occurred as a result of cracking in the gold layer induced by plastic deformation in the polymer matrix.

Micrographs from the woven carbon fibre reinforced epoxy indicated that the mode of failure was again dependent upon the rate at which the material was loaded. Characterising the crack tip damage mechanisms in composites of this type is problematic since the local strain field and damage type depends upon the position of the 900 fibres relative to the starter defect. A number of large shear cracks are apparent in the resin-rich region ahead of the precrack. At higher rates of loading, these cracks were much smaller and more localised. Clearly, the presence of large crack at the tip of the starter crack results in a significant loss in the interlaminar properties. At high rates of loading, these cracks do not have time to extend and propagate and this is reflected in the higher fracture properties determined under these conditions.

Although the precise modes of failure in the two composites are slightly different, it is apparent that damage is more severe in specimens tested at

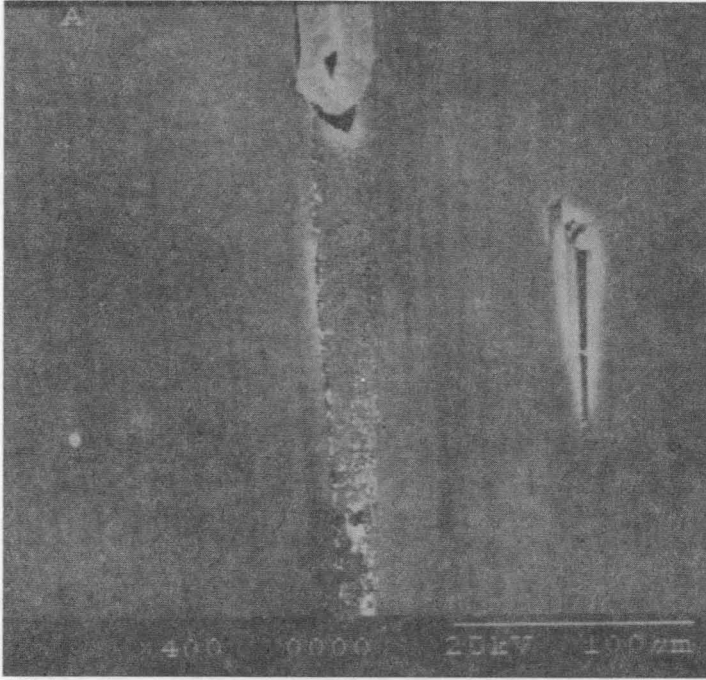


FIGURE 8. Crack tip region in a carbon fibre reinforced PEEK specimen tested at 3 m/s

very low strain rates. This finding appears to support the experimental observations where increasing the crosshead displacement rate was shown to yield an increase in the measured values of G_{IIc} . Further work is currently underway to relate the basic viscoelastic properties of the polymer matrix to the fracture behaviour of the composite.

CONCLUSIONS

High performance composite materials exhibit distinct rate sensitive characteristics when tested under mode II loading conditions. It has been shown that the woven carbon fibre reinforced epoxy exhibits interlaminar fracture properties comparable to those of a tough thermoplastic composite. The experimental evidence has shown that the values of G_{IIc} for carbon fibre reinforced PEEK and the woven carbon fibre reinforced epoxy increase significantly with increasing loading rate until it reached 3mm/min. A novel test geometry has been developed to study mode II failure mechanisms in these materials. Using the double end-notched flexure specimen, it has been shown that damage in the crack tip regions at these low loading rates appears to explain the relatively low values of G_{IIc} measured under these conditions.

REFERENCES

- Bradsky, G.V., Chivers, R.A., Crick, R.A. & Turner, R.M. 1993. Interlaminar fracture toughness of a range of continuous fibre/PEEK composites. *Composites Science and Technology* 47: 75 - 81.
- Cantwell, W.J. & Morton, J. 1989. Comparison of the low and high velocity impact response of CFRP. *Composites* 20 (6): 545-551.
- Davies, P., Cantwell, W.J., Moulin, C. & Kausch, H.H. 1989. A study of the delamination resistance of IM6/PEEK. *Composites, Composites Science and Technology* 36: 153-166.
- Davies, P. 1990. *Protocol for Interlaminar fracture toughness testing of composites*. European Structural Integrity Society (ESIS), Polymer and Composite Task Group, IFREMER, France.
- Hashemi, S. , Kinloch, A.J. & Williams, J.G. 1990. The effects of geometry, rate and temperature on the mode I, Mode II and Mixed-mode I/II Interlaminar Fracture of Carbon-fibre/Poly(ether-ether ketone) composites. *Journal of Composite Materials* 24: 918-957.
- Maikuma, H., Gillespie, J.W. & Wilkins, D.J. 1990. Mode II Interlaminar fracture of the center notch flexural specimen under impact loading. *Journal of Composite Materials* 24: 124-149.
- Smiley, A.J. & Pipes, R.B. 1987. Rate sensitivity of Mode II interlaminar fracture toughness in Graphite/Epoxy and Graphite/PEEK *Composite Materials. Composites Science and Technology* 29 (1): 1-15.
- Sue, H.J., Jones, R.E. & Garcia-Meitin, E.I. 1993. fracture behaviour of model toughened composites under Mode I and Mode II delaminations. *Journal of Composite Materials* 28: 6381-6391.
- Sue, H.J., Garcia-Meitin, E.I., Pickelman, D.M. & Yang, P.C. 1990. *Toughened Plastics: Science and Engineering*, ACS, Vol. 233, edited by C.K. Riew, in press.
- Todo, M., Takahashi, K., Beguelin, P. and Kausch, H.H. 1997. Effect of strain rate on tensile fracture behaviour of fibre reinforced polyamide composites, *Proceedings of 11th International Conference on Composite Materials* 2: 405-414.
- Wang, H. & Vu-Khanh, T. 1995. Fracture mechanics and mechanisms of impact-induced delamination in laminated composites. *Journal of Composite Materials* 29(2): 156-178.
- Yaniv, G. & Daniel, I.M. 1988. Composite materials : Testing and design. *American Society for Testing and Materials*, STP 972: 241-258.
- Yee, A.F. 1986. Toughened composites. *American Society for Testing and Materials* STP 937: 383.

Rozli Zulkifli
 Department of Mechanical & Materials Engineering
 Faculty of Engineering
 Universiti Kebangsaan Malaysia
 43600 UKM Bangi,
 Selangor D.E. Malaysia

W.J. Cantwell & Matt. Blyton
 Department of Materials Science and Engineering
 University of Liverpool
 Liverpool L69 3BX
 United Kingdom